Inorganica Chimica Acta 525 (2021) 120488

Contents lists available at ScienceDirect

Inorganica Chimica Acta

journal homepage: www.elsevier.com/locate/ica

Research paper

Electrochemical reactor for sustainable transformation of bio-mass derived allyl alcohol into acrylate and pure hydrogen

Maria Vincenza Pagliaro [a], Hamish Andrew Miller [a,*], Marco Bellini [a], Benedetto Di Vico [a], Werner Oberhauser [a], Giovanni Zangari [b], Massimo Innocenti [c], Francesco Vizza [a,*]

[a] *Institute of Chemistry of Organometallic Compounds – National Research Council of Italy (ICCOM-CNR), Via Madonna del Piano 10, 50019 Sesto Fiorentino (Florence), Italy*

[b] *University of Virginia, Dept Mat Sci & Engn, Charlottesville, VA 22904 USA*

[c] *University of Florence, Dept Chem Ugo Schiff, Via Lastruccia 3, I-50019 Sesto Fiorentino, FI, Italy*

ARTICLE INFO

Keywords:
Electrochemical reforming
Electrolysis
Hydrogen
Pd-CeO_2/C
Acrylic acid
Allyl alcohol

ABSTRACT

Acrylic acid is widely used in the chemical, polymer, cosmetic and food industries. Typically, it is produced through processes with a high environmental impact. In this paper, we demonstrate the co-production of the potassium acrylate salt and hydrogen gas from allyl alcohol in a liquid flow fed anion exchange membrane electrolysis cell operating at 60 °C and ambient pressure. We compare in electrolysis cell tests, two electro-catalysts Pd/C and Pd-CeO_2/C evaluating the activity and selectivity for acrylate production. Electrolysis cell parameters are tuned obtaining a maximum conversion of allyl alcohol of 96% and a selectivity to acrylate of 50% at an operating cell voltage of 1 V. Operating at a lower cell potential (0.7 V) the selectivity for acrylate increases to 74%. Hydrogen gas is produced in the separated cathode compartment at an energy cost of 26 KWh kg^{-1}_{H2}, which is around half when compared to state-of-the-art water electrolyzers. The electrochemical oxidation mechanism of allyl alcohol is also studied and discussed, providing for the first time an insight into the pathways for formation of acrylate with respect to the other principle oxidation products (propionate and 3-hydroxypropionate).

1. Introduction

Acrylic acid (AcA) is a precursor to acrylic based polymers, useful for their absorbent properties and used in a wide range of applications such as surface coatings, paint formulations, textiles, adhesives, paper treatment, leather, fibers and detergents [1–3]. Worldwide production of acrylic acid was 4.5 million tons in 2012 with a growing demand of 4% per year [3]. AcA is currently produced from crude oil through the two-step gas-phase oxidation of propylene, producing acrolein as an intermediate [3]. The growing industrial demand for AcA, combined with the need for a progressive reduction of dependence on fossil fuels, means we need new production processes based on renewable biomass resources. Glycerol (Gly), is a major byproduct of the biodiesel industry, has attracted attention as a precursor for the production of various chemicals (propanediol, lactic acid, acrolein, allyl alcohol) and their consequent conversion to AcA [3,4]. For example, Li and Zhang [5] report a novel two-step method through glycerol deoxydehydration (DODH) using formic acid to form allyl alcohol (AA), followed by oxidation to AcA in the gas phase over Mo – V – W – O catalysts. An overall AcA yield of 80% was achieved. The current process of oxidizing AA to AcA involves high temperatures (up to 340 °C in the second step), the use of pure oxygen, and the co-production of a CO and CO_2 waste mixture. More recently, Ueda et al. studied the oxidation of AA using four kinds of crystalline (orthorhombic, trigonal, tetragonal and amorphous) MoVO catalysts, and investigated the active sites for the reaction. The maximum yields of AcA were 73% for the orthorhombic Mo_3VOx catalyst and 72% for the trigonal Mo_3VOx catalyst at 350 °C [3,6]. Kim and Lee have developed the liquid-phase oxidation of AA to AcA using an Au-CeO_2 catalyst; a 92% yield of AcA, at 25 °C and 10 bar O_2 pressure in the presence of NaOH, was obtained [7]. In this work, we demonstrate a process for the preparation of the potassium salt of acrylic acid (potassium acrylate) from AA through electrochemical oxidation in a membrane electrolysis flow cell at 60 °C without the need for high pressure O_2. As shown in our previous works, this technology presents numerous advantages combining the production of valuable chemicals from biomass-derived starting materials with the production of clean

---

* Corresponding authors.
E-mail addresses: hamish.miller@iccom.cnr.it (H.A. Miller), francesco.vizza@iccom.cnr.it (F. Vizza).

https://doi.org/10.1016/j.ica.2021.120488
Received 30 March 2021; Received in revised form 27 May 2021; Accepted 31 May 2021

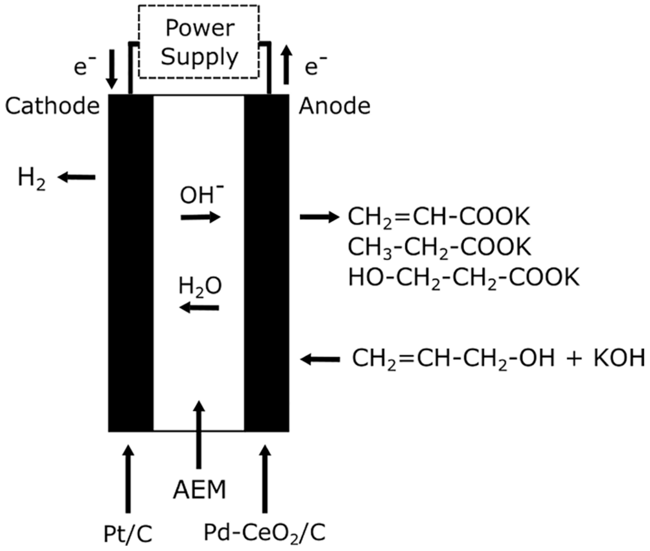

Fig. 1. Schematic representation of the electrolysis cell.

hydrogen at low temperature and atmospheric pressure (see Fig. 1) [8–11].

The selectivity of the oxidation reaction for the desired product may be tuned by varying the cell operating parameters (e.g. temperature and anode potential). The nature of the anode catalyst may also influence the oxidation selectivity [12]. To this regard, we compare two electrocatalysts (Pd/C and Pd/C-CeO_2) at the anode, evaluating the activity and product selectivity. The Pd-CeO_2/C catalyst has been shown to exhibit enhanced alcohol oxidation activity [9,11]. The CeO_2 promotes the formation at low potentials of species adsorbed on Pd, (e.g. Pd^I-OH_{ad}), that are involved in alcohol oxidation [13]. Electrolysis cell parameters are also tuned to favor the formation of acrylate with respect to the main by-products (propionate and 3-hydroxypropionate) obtaining a maximum conversion of AA of 96% and a selectivity to Ac of 50% at a constant operating voltage of 1 V. At the same time pure hydrogen is produced at cathode side with an energy consumption of only 26 KWh kg_{H2}^{-1}, about the half when compared to state of the art water electrolyzers [14]. To the best of our knowledge this is the first time AA has been used as substrate in a complete electrochemical reforming cell with the objective of producing acrylate. The reaction mechanism was investigated, highlighting the existence of two separated oxidation processes: a 4 e^- electrochemical path for the oxidation of AA to AcA and the simultaneous isomerization of allyl alcohol to propionaldehyde, which is oxidized to propionate through a 2 e^- path.

2. Experimental

2.1. Materials

Carbon black (Vulcan XC-72) was purchased from Cabot Corp., USA. All metal salts and reagents were purchased from Aldrich and used without further purification. A commercial 40 wt% Pt/C catalyst was used as (Hydrogen Evolution) cathode catalyst, while the Pd/C and Pd/C-CeO_2 anode catalysts were prepared as already reported in our previous works [15]. The anion exchange membrane used was A-201, obtained from Tokuyama Corp. (Japan).

2.2. Electrochemical tests

The electrochemical measurements were carried out using a Parstat 2273 potentiostat–galvanostat (Princeton Applied Research) equipped with a Model 616 Rotating Disk electrode (PAR-Ametek). A 5 mm ($A = 0.1963\ cm^2$) Teflon potted glassy-carbon disk electrode tip (PINETM) was used as substrate for the deposition of the catalyst ink. Before the deposition, the glassy-carbon surface was polished with different CT diamond suspensions featuring progressively smaller particle size (1 μm, 0.25 μm, 0.1 μm) and finally washed with distilled water. The catalyst ink is composed of Pd/C or Pd/C-CeO_2 (7 mg) in a 50:50 water/ethanol solution (600 mg water and 600 mg ethanol) with about 12 mg of a 5% Nafion® perfluorinated resin solution. The resulting suspension was sonicated for 1 h with a FALC sonic bath to reach a uniform suspension. The catalyst film was prepared by casting 5 μL of the catalyst ink onto the glassy-carbon electrode. The exact amount of ink deposited was determined using an analytical balance. The final metal loading on the electrode is between 4 and 6 μg. Each electrode was dried for 30 min before and finally it was mounted on the rotating disk electrode shaft and immersed into the electrolyte solution. The reference electrode was a commercial Ag/AgCl/KCl (1 M). The counter electrode was a platinum gauze enclosed in a glass tube with porous bottom. All the potentials reported are versus the reversible hydrogen electrode (RHE). The CV experiments were undertaken in static N_2 saturated aqueous solutions of both 0.5 M KOH and 0.5 M KOH + 0.5 M allyl alcohol. All the solutions were prepared with Millipore water (18 MΩ*cm) provided by a milli-Q labo apparatus (Nihon Millipore Ltd.). Cyclic voltammetry was undertaken from 0 to 1.4 V (vs RHE) at a scan rate of 10 mV s^{-1}.

2.3. Electrolysis cell tests

The MEAs (membrane electrode assemblies) were composed of a nickel foam support coated with either the Pd/C or Pd-CeO_2/C catalyst as anode, a commercial Tokuyama A-201 anion-exchange membrane, and a commercial 40 wt% Pt/C (Aldrich) catalyst supported on carbon cloth as cathode. The anode ink was prepared by mixing the catalyst with a 5% aqueous suspension of PTFE to form a dense catalyst paste which is spread onto a 5 cm^2 Ni-foam support (Heze Tianyu Technology Development Co., China) in order to obtain a catalyst coated electrode with a Pd metal loading of 1 mg cm^{-2}. The cathodic ink was prepared in a 5 mL high density polyethylene vial, mixing 200 mg of the commercial Pt (40 wt%)/C in 450 mg of distilled water, 790 mg of 1-propanol and 1.56 g of the ionomer Nafion® (5 wt% in 2-propanol). The mixture was suspended with three pulses of ultrasound, 20 W power at the frequency of 20 kHz (Bandelin Sonor pulse UW 2200 SERIES). Finally, this paste was spread onto a carbon cloth W1S1005 (CeTech Co. Ltd.) gas diffusion layer, with a Meyer rod (n°150) obtaining a 0.4 mg cm^{-2}Pt loading.

The electrochemical flow cell was purchased from Scribner-Associates (USA). The MEAs were assembled by mechanically pressing together the anode, cathode and membrane within the cell hardware. The cell temperature was regulated at 60 °C using a Scribner 805e fuel cell station. The aqueous fuel solution (0.5 M KOH + 0.5 M allyl alcohol) was delivered to the anode at 1 mL min^{-1}. Voltage scans and galvanostatic curves were determined using an ARBIN BT-2000 5A-4 channels instrument. Polarization experiments were recorded by applying a linear voltage ramp with a 10 mV s^{-1} scan rate between 0.2 and 1.2 V. Chronopotentiometry experiments were performed applying a constant electrolysis current of 125 mA until the cell voltage reached the value of 1.2 V. Amperometry experiments were also performed tuning cell potential values from 0.4 V to 1 V. The hydrogen generation flow was recorded by a Bronkhorst EL-FLOW mass flow meter model F-101C-002-AGD-11-V with a maximum H_2 flow rate of 3 mL min^{-1}.

2.4. Model reaction investigations and product analysis

Model catalytic reactions were performed in a PTFE-coated, stainless steel autoclave (volume 50 cm^3), equipped with a magnetic stirrer and temperature and pressure controllers. The fuel solutions after each experiment were quantitatively and qualitatively analyzed by $^{13}C\{^1H\}$ NMR spectroscopy and HPLC. A UFLC Shimadzu Chromatograph equipped with refraction index detector (RID) was used; the column is a GRACE- Alltech OA-1000 Organic Acids (300 mm × 6.5 mm),

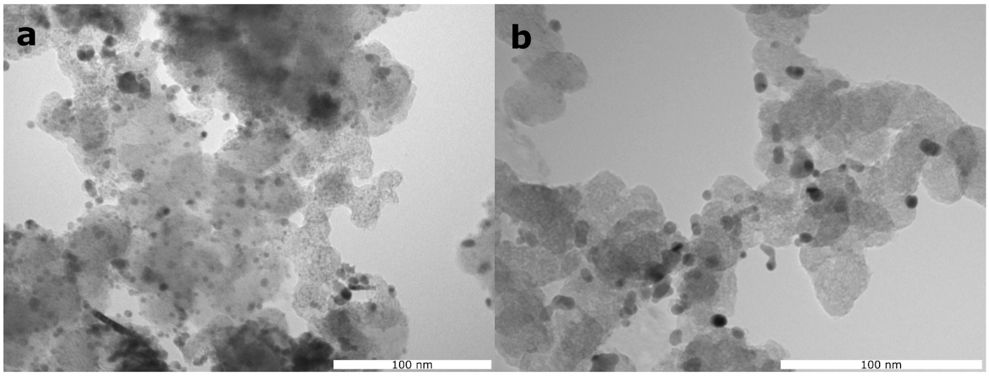

Fig. 2. TEM images of representative portions of (a) Pd/C-CeO$_2$ and (b) Pd/C.

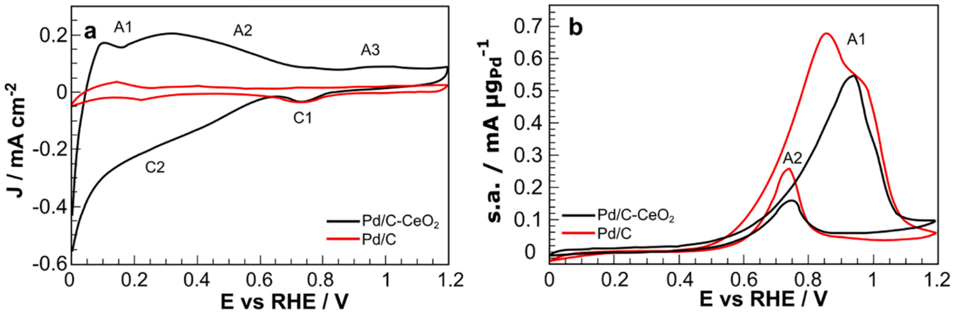

Fig. 3. CVs in N_2 saturated aqueous solutions of (a) 0.5 M KOH (b) 0.5 M allyl alcohol + 0.5 M KOH at 10 mV s^{-1}.

thermostated at 65 °C. The eluent is 0.01 N H_2SO_4; and the eluent flow is 0.4 mL min^{-1}. NMR spectra were acquired with a Bruker Avance DRX 400 spectrometer. Chemical shifts (δ) are reported in ppm relative to TMS. Deuterated solvents (Sigma-Aldrich) used for NMR measurements were dried with activated molecular sieves; 1,4-dioxane was used as internal standard for product quantification.

3. Results and discussions

The Pd/C and Pd/C-CeO$_2$ anode electrocatalysts with 10 wt% Pd have been fully characterized in our previous reports through XRD, chemisorption, XAS and HR-TEM.[16] Representative TEM images of both catalysts are shown in Fig. 2. As demonstrated in our previous studies, the ceria in the support plays a key role in promoting the formation, at low potentials, of hydroxide species adsorbed on Pd (Pd^{I}–OH$_{ad}$) that leads to enhanced electrocatalytic activity. Under strongly alkaline conditions (pH ≥ 13), on palladium (Pd) electrocatalysts, alcohols are generally partially oxidized to carboxylate compounds without formation of CO_2.[12] The Pd/C-CeO$_2$ catalyst readily transforms a ranged of alcohols into carboxylates in the electrochemical reforming cell.[9,11] In this study Pd-CeO$_2$/C is compared to Pd/C with AA as substrate.

3.1. Electrochemical study of allyl alcohol oxidation

The electrochemical characteristics of Pd/C and Pd/C-CeO$_2$ were investigated by cyclic voltammetry (CV) in both 0.5 M KOH (Fig. 3a) and 0.5 M allyl alcohol + 0.5 M KOH (Fig. 3b).

The CVs of Pd/C and Pd/C-CeO$_2$ were firstly obtained in N_2 saturated 0.5 M KOH (Fig. 3a) and show features characteristic of Pd-centered transitions that have been assigned by comparison with literature data [11,15,16]. On the forward anodic scan (0 to 1.4 V), there are three transitions (A1-A2-A3). The broad peak A1, centered at 0.4 V, is due to the oxidative desorption of hydrogen. The shallow approach to the limiting current at about 0.6 V (A2) is ascribed to the formation of palladium hydroxides. This is followed by the formation of an oxide layer (A3) on the palladium surface that is associated with a gentle increase in the anodic current density. On the reverse cathodic scan (1.4 to 0 V), the peak at 0.7 V (C1) is assigned to the reduction of Pd oxides, whereas the broad cathodic feature at potentials between 0.5 and 0.2 V

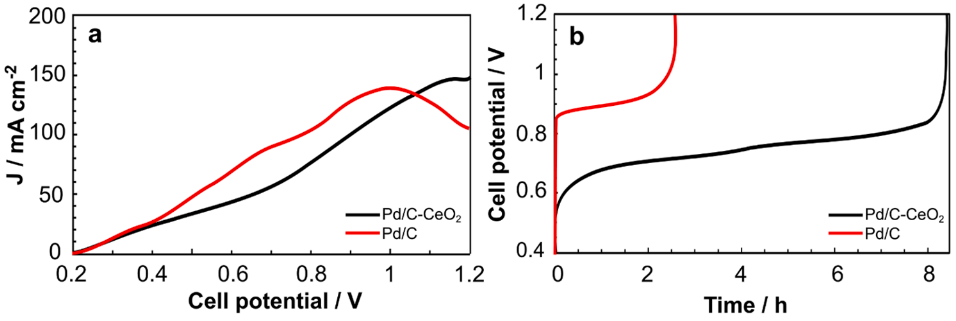

Fig. 4. MEA (1): (a) potentiodynamic experiments (b) galvanostatic experiments at 50 mA cm^{-2}. Cell temperature 60 °C.

Table 1
Electrolysis data with allyl alcohol.

TEST	Type of experiment	[@]Electrochemical Conversion/%	[$]Selectivity/%			H_2/L min^{-1} m^{-2}	Energy Consumption /KWh kg$_{H2}$
			**Ac*	**Prp*	**3-Hp*		
Pd/C-CeO$_2$							
(1)	J_K = 50 mA cm^{-2}	64	41.3	50.4	8.3	1.17	20.2
(2)	V_k = 0.4 V	14	44.3	54.1	1.6	0.25	10.8
(3)	V_k = 0.7 V	63	43.0	52.6	4.4	1.15	18.7
(4)	V_k = 1 V	96	42.7	53.2	3.1	1.95	26.8
Pd/C							
(5)	J_K = 50 mA cm^{-2}	19	34.3	63.3	2.4	3.12	24.7
(6)	V_k = 0.4 V	26	34.2	22.7	43.1	0.01	10.7
(7)	V_k = 0.7 V	61	73.9	16.7	9.4	0.98	18.7
(8)	V_k = 1 V	96	50.1	49.8	1.1	1.54	26.8

°Galvanostatic (constant current density j_k), Potentiostatic (constant voltage V_k);

*Acrilate (Ac), Propionate (Prp), 3-hydroxypropionate (3-Hp);

[@] Considering the double oxidation pathway at 4 and 2 e$^-$, and a propionate/acrylate ratio of 1.2;

[$] Data from $^{13}C\{^1H\}$ NMR spectroscopy and HPLC analysis.

(*C*2) is attributed to hydrogen adsorption. The CV of Pd-CeO$_2$/C has also the characteristic underlying redox features of the CeO$_2$ part of the support that are visible in the region 0 to 0.6 V (RHE).

The electrochemical activity of Pd/C and Pd/C-CeO$_2$ towards the electrooxidation of allyl alcohol was also investigated by cyclic voltammetry in a solution of 0.5 M AA + 0.5 M KOH. The forward anodic scans reported in Fig. 3b have the onset potential for AA oxidation at approximately 0.5 V (vs RHE) and the recorded oxidative current density increases continuously with increasing potential. The subsequent current decrease after the peak (0.8 to 1.0 V) corresponds to the progressive formation of an inactive palladium oxide layer [17]. In the reverse scan there is e a small peak in current density (A2) at around 0.7 V, due to the reactivation of the palladium surface (removal of surface oxides) that are active for allyl alcohol oxidation. The electrochemical characteristics of allyl alcohol oxidation by Pd/C and Pd/C-CeO$_2$ determined here are consistent with the activity profile with a range of other alcohols previously reported (e.g. ethanol, methanol, ethylene glycol, glycerol, 1,2-propandiol, 1,3-propandiol and 1,4-butandiol) [9,11].

3.2. *Electrolysis cell testing*

The anode, membrane, and cathode were pressed together within the cell hardware to form the membrane electrode assembly (MEA) for testing. The anode compartment of the cell was fed by recycling 50 mL of aqueous solutions of 0.5 M allyl alcohol + 0.5 M KOH while the cathode compartment was connected to a flow meter to measure the H_2 production. The cell performance was firstly measured using potentiodynamic scans at a cell temperature of 60 °C. The potentiodynamic scans (examples are shown in Fig. 4a) were performed from 0 to 1.2 V at 10 mV s^{-1}. The curves reach approximately 150 mA cm^{-2} maximum current density at 1 V for Pd/C and 1.2 V for Pd-CeO$_2$/C respectively. Under the same cell conditions higher current densities have been obtained with other alcohols, demonstrating the slower kinetics of AA electrooxidation due to the strong adsorption of intermediates, as will be discussed in detail below (see Table 2 for comparison). For example, Pd-CeO$_2$/C achieved up to 400 mA cm^{-2} at 1 V for 1,3-propandiol and Ethylene Glycol oxidation under the same conditions [11]. The current density drops after 1 V for Pd/C while for Pd-CeO$_2$/C the CD increases up to 1.2 V. Demonstrating a poisoning of the Pd/C catalyst by progressive oxidation that does not occur below 1 V on Pd-CeO2/C. Pd-CeO2/C has been shown to be more stable under potential cycling in alkaline media [16]. A constant current experiment (50 mA cm^{-2}) using a single batch of fuel (50 cm3) was run for each catalyst. From Fig. 4b it is clear that the Pd-CeO2/C catalyst is more stable able to transform 64% of the AA present compared to 19% for the Pd/C catalyst.

Table 2
Comparison of electrochemical reforming data with Pd-CeO$_2$/C at the anode at T_{cell} of 60 °C. 1,2-P = 1,2-propandiol, 1,3-P = 1,3-propandiol, EG = ethylene glycol, 1,4-B = 1,4-butanediol. Data from refs. 9 and 11 were obtained at a current density of 30 mA cm^{-2}.

Fuel	J_{max} @ 1 V (mA cm^{-2})	H_2 (mmol)	Energy Consumption (kWh kg^{-1}$_{H2}$)	Conversion (%)	Ref.
HCOOK	355	46	6.0	77	9
Methanol	425	85	13.4	81	9
Ethanol	444	68	14.5	96	9
1,2-P	420	107	18.9	77	9
EG	336	96	16.9	71	9
Glycerol	372	92	15.6	52	9
1,4-B	395	102	17.5	67	9
1,3-P	400	93	16.3	68	11
AA	150	40	20.2	64	This work

In order to identify and quantify the ally alcohol electrooxidation product distribution for each catalyst, the fuel solutions after constant current density experiments (50 mA cm^{-2}) were quantitatively and qualitatively analyzed by $^{13}C\{^1H\}$ NMR spectroscopy and HPLC. The formation of three main products was detected and quantified: acrylate, propionate and 3-hydroxypropionate. Additionally, the electrical energy consumption of the process was determined from the integration of the instantaneous charging power over the duration of the galvanostatic experiment. The H_2 produced during each run was determined using a flow meter connected to the outlet of the cathode compartment. Results are summarized for all tests in Table 1.

To study the AA conversion efficiency and selectivity to AcA for each catalyst, a series of potentiostatic (constant cell voltage) experiments were carried out applying three cell potentials: TEST (2) which operates at 0.4 V, TEST (3) at 0.7 V and TEST (4) at 1 V. The corresponding potentiostatic curves are shown in Fig. 5a and 5b and their extrapolated electrochemical data are reported in Table 1. At the highest operating voltage of 1 V, the catalysts show the highest activity for AA oxidation, starting at 140 and 100 mA cm^{-2} current density for Pd-CeO$_2$ and Pd/C respectively. The AA total conversion at 1 V reaches 96% for both catalysts (Table 1). This result is consistent with the cell voltage scan experiments (Fig. 2a) where the cell exhibits the maximum electrochemical activity for AA oxidation at approximately 1 V. At lower cell potentials, significantly lower current densities and conversion efficiencies are observed. The current density decreases over time due to

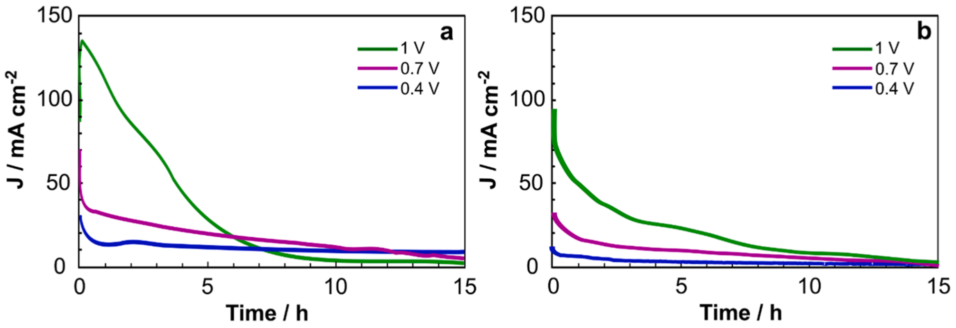

Fig. 5. Potentiostatic experiments carried out at cell voltages of 0.4 V, 0.7 V, and 1 V for the cell equipped with (a) Pd/C-CeO$_2$ and (b) Pd/C anode.

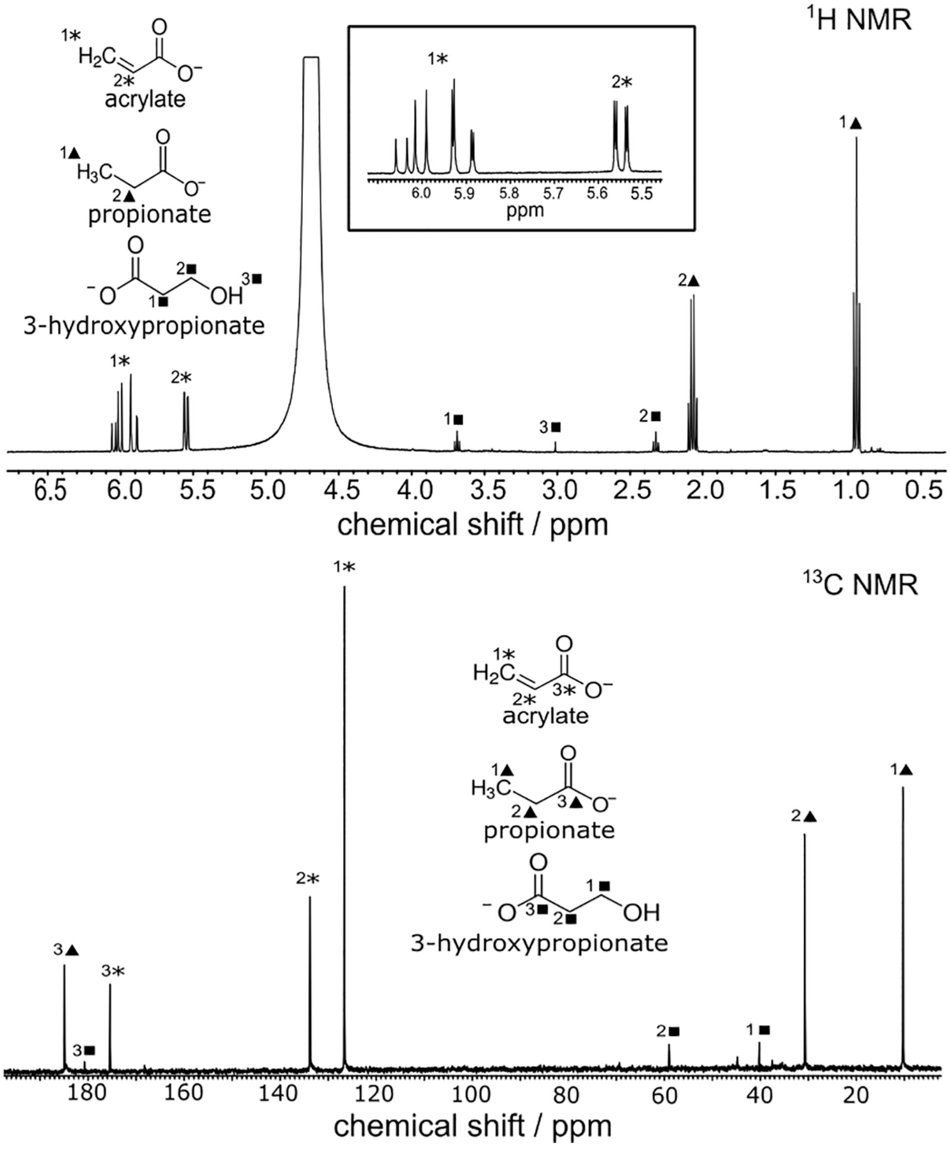

Fig. 6. ^{1}H NMR and ^{13}C NMR spectra of the product solution after a typical potentiostatic experiment @1 V.

the progressive consumption of AA, which is oxidized to Acrylate and other products. The higher energy introduced to the cell at 1 V is what forces the reaction to a higher conversion (KWh Kg^{-1} 26.8 vs 10.8 @ 0.4 V).

The fuel solutions at the end of each experiment were quantitatively and qualitatively analyzed by ^{13}C{^{1}H} NMR spectroscopy and HPLC to determine the AA oxidation products. The results are summarized in Table 1. Acrylate (Ac) and propionate (Prp) are the main products detected together with a small amount of 3-hydroxypropionate (3-Hp). Typical NMR spectra for the AA fuel solutions after the potentiostatic experiments are presented in Fig. 6. The origin of each peak was determined by comparison with standards. The concentration of each compound was calculated by the HPLC peak area through the use of predetermined calibration curves. From Table 1, the product

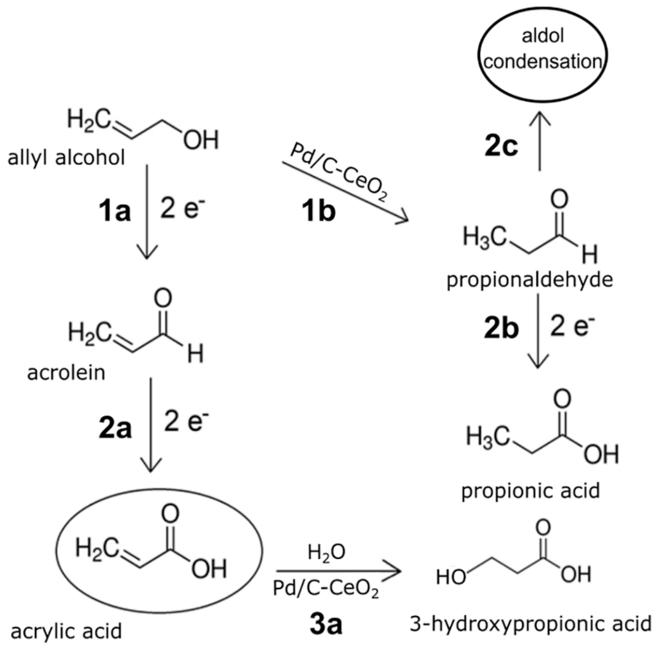

Scheme 1. Allyl alcohol oxidation mechanism.

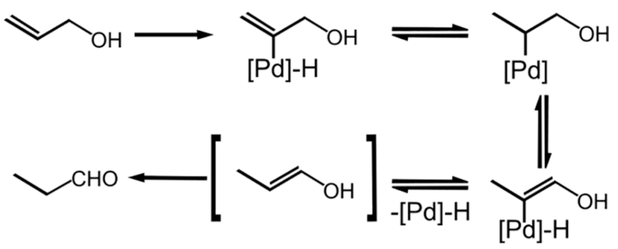

Scheme 2. Mechanism for the isomerization of allyl alcohol[18].

distribution of Pd-CeO$_2$/C catalyst remains relatively constant regardless of the cell voltage with the ratio Ac:Prp of approximately 45:55. By comparison the amount of acrylate produced by the Pd/C catalyst is affected by the working cell voltage. At low cell voltage acrylate formation is not favored while at 0.7 V selectively for acrylate reaches 74%.

3.3. Study of the allyl alcohol electrooxidation reaction mechanism

Both of the co-products identified during the electrolysis of AA (PrP and 3-Hp) cannot be formed from solely electrochemical reactions. To help us understand better the reaction mechanism and the origin of formation of propionate and 3-hydroxypropionate during the electrolysis, model experiments were performed in a sealed 50 cm^3 stainless steel pressure autoclave with a PTFE® liner. The first experiment (TEST A) was carried out with 100 mg of Pd/C-CeO$_2$ powder in 25 cm^3 of an aqueous solution of 0.5 M acrylate + 0.5 M KOH, at 60 °C for 10 h. This model of reaction was performed in order to verify if acrylate could undergo the addition of a water molecule to the C—C double bond catalyzed by Pd/C-CeO$_2$ in alkaline conditions with the resultant formation of 3-hydroxypropionate (step **3a** of Scheme 1). NMR analysis after the experiment confirms the formation of 3-hydroxypropionate, through the "**a**" route for the formation of 3-hydroxypropionate from allyl alcohol. The acrylate formed electrochemically (1a + 1b) is then transformed to 3-hydroxypropionate through a non-electrochemical catalytic process.

Propionate which is also formed, cannot derive from a direct oxidation electrochemical process from allyl alcohol. Using data from the literature regarding palladium hydroxide catalyzed isomerization of primary allyl alcohols to aldehydes (scheme 2) [18–22,18–22] we hypothesized a second double step route: the first step (**1b** of scheme 1) involves the isomerization of allyl alcohol to propionaldehyde, and a second step (**2b**) involves a 2 e- electrochemical process of oxidation to propionate. To demonstrate that the formation of propionate occurs through the "**b**" pathway, we performed two tests (TEST B and TEST C) in the autoclave. Both tests were carried out with 100 mg of Pd/C-CeO$_2$ powder in 25 cm^3 of an aqueous solution of 0.5 M allyl alcohol (**TEST B**) and 0.5 M allyl alcohol + 0.5 M KOH (**TEST C**), at 60 °C for 5 h. At the end of experiments, both the solutions were analyzed through ^{1}H NMR to verify the formation of propionaldehyde. The ^{1}H NMR spectrum of

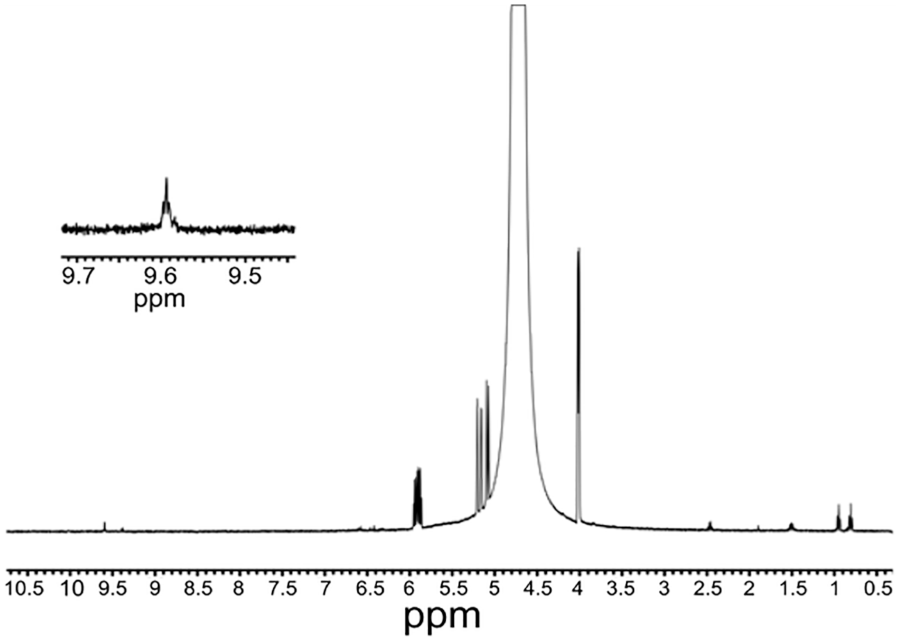

Fig. 7. ^{1}H NMR spectra of the TEST B aqueous solution of 0.5 M allyl alcohol after a 5 h reaction at 60 °C, which evidences the formation of propionaldehyde at 9.6 ppm.

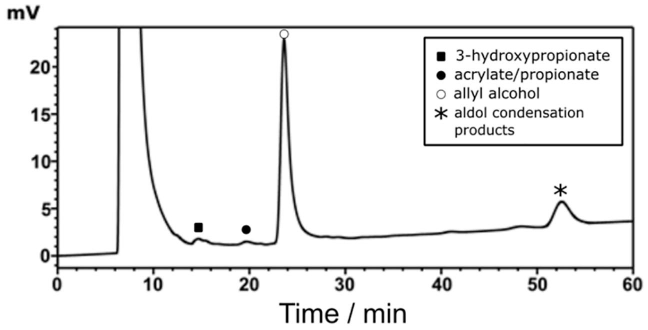

Fig. 8. HPLC trace of a 0.5 M solution of 0.5 M allyl alcohol and 0.5 M KOH, fed to the cell at OCV and recycled at 60 °C for 18 h.

TEST B solution shows the typical triplet proton signal at 9.6 ppm that confirms the presence of the aldehyde (Fig. 7); Analysis of the TEST C solution did not show the presence of aldehyde. This is due to the instability of propionaldehyde in alkaline media (pH 13.7) to fast reaction with allyl alcohol through aldol condensation (Scheme 1 step **2c**). HPLC analysis of the TEST C solution, showed the appearance in the chromatogram of a large peak at 53 min that we assigned to various aldol condensation products. The formation of aldol condensation products was also verified in the electrolysis cell, fueling a 0.5 M allyl alcohol + 0.5 M KOH solution to the cell at open circuit voltage (no current passed to the cell) for 18 h at 60 °C. The HPLC trace of the recovered solution shows the presence of the same aldol condensation products peak found for TEST C (Fig. 8). On the contrary, at operating conditions of 1 V (high current density), the propionaldehyde is rapidly electro-oxidized to propionate, limiting the collateral aldol condensations.

3.4. Discussion

This study has demonstrated that allyl alcohol can be readily oxidized to acrylate in an electrolysis cell with the combined production of H_2. Hydrogen is produced in the membrane separated cathodic compartment and can be fed directly to a fuel cell to be transformed into electrical energy. Using the cell running at 1 V as an example, the energy cost of the hydrogen produced is 26.8 KWh kg_{H2}^{-1} (Table 1). The hydrogen produced has an energy content of 33 KWh kg_{H2}^{-1} (LHV).[23 If this hydrogen is fed to a state of the art PEM-FC stack with an energy efficiency of approximately 50%, a 16.5 KWh kg_{H2}^{-1} electrical energy output will be generated. This energy can be recycled back to the AA electrolysis process. In this way more than half of the energy cost of the electrolysis is recovered.

There are additional advantages of this electrolysis process, including a low temperature and ambient pressure operation, as well as the possibility to obtain H_2 at high pressures (up to 10 bar). In addition, no pure O_2 is required for the oxidation reaction: the oxygen required by the process is here obtained from the water reduction at the cathode that produces hydroxyl anions, which cross the anion exchange membrane to the anode where they are involved in the oxidation of the alcohol (Fig. 1). Table 2 compares literature data for alcohol electrochemical reforming with the Pd-CeO_2/C anode catalyst. The conversion efficiencies are related to constant current tests rather than fixed cell potential tests. The data shows how the nature of the substrate determines the energy cost and conversion efficiency. Generally, the simpler alcohols (e.g. methanol, ethanol) consume less energy and are more kinetically favored. AA demonstrates slower kinetics and higher energy requirement compared to the other alcohols reported.

At a cell potential of 1 V the conversion of allyl alcohol is close to 100%. The selectivity for acrylate is around 43%. The competing process which suppresses the selectivity has been identified as the Pd catalyzed isomerization of AA to the corresponding aldehyde which is then oxidized electrochemically to proprionate. Strategies to prevent the isomerization of AA will require the development of alternative catalysts that do not catalyze this parasitic reaction. In the case of Pd/C improved selectivity for acrylate can be obtained by setting the cell potential at 0.7 V although the conversion efficiency drops to 60%. We are currently investigating nanostructured Pd-M alloy materials as alternative catalysts to this end. Regarding the stability of the MEA we have performed 3 consecutive galvanostatic experiments with both Pd-CeO_2/C and Pd/C catalysts. After each run the used fuel solution was replaced by a fresh batch. The cell voltage was monitored during each experiment (Fig. 9). There does not appear to be significant degradation in performance over the three experiments. To determine the future economic and environmental feasibility of acrylate production by electroreforming will require a study of long term stability of the catalyst materials in scaled up processes along with dedicated LCA studies.

4. Conclusions

In this work, we demonstrate the first study of acrylate production by the oxidation of allyl alcohol in an electrolysis cell. The process has a low energy cost, operates at mild temperature and at ambient pressure, and it also produces clean and pure hydrogen that can be used to produce electrical energy in a fuel cell. A nanostructured Pd/C-CeO_2 was used as anode material, which presents enhanced activity and stability for alcohol electrooxidation under alkaline conditions, providing a maximum conversion of AA of 96% and a selectivity to Ac of 43.0% at a constant cell operating voltage of 1 V. An equivalent Pd/C catalyst shows improved selectivity at 0.7 V (74%). To make the process a valid alternative to current petrochemical-based technologies, the selectivity for the formation of acrylate compared to the other main oxidation products (propionate and 3-hydroxypropionate) must be optimized. A detailed reaction mechanism investigation was performed in this study that will help in finding strategies for improving the selectivity for acrylate.

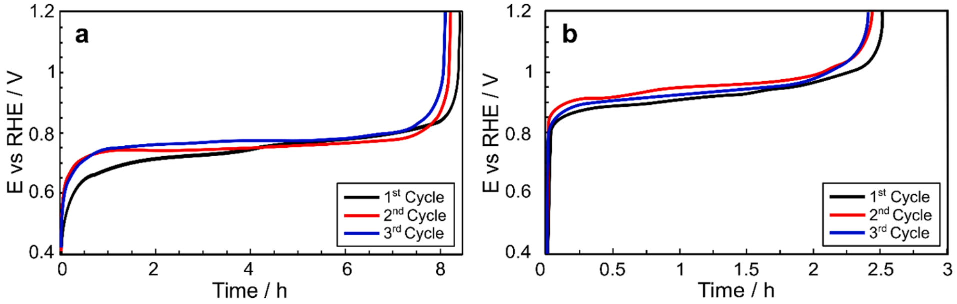

Fig. 9. Three consecutive galvanostatic experiments (50 mA cm^{-2}) carried out at 60 °C with three batches of fresh fuel solution (50 mL aqueous solution of 0.5 M allyl alcohol + 0.5 M KOH) (a) Pd-CeO_2/C and (b) Pd/C.

CRediT authorship contribution statement

Maria Vincenza Pagliaro: Investigation, Visualization, Formal analysis. **Hamish Andrew Miller:** Investigation, Formal analysis. **Marco Bellini:** Investigation, Formal analysis. **Benedetto Di Vico:** Investigation, Formal analysis. **Werner Oberhauser:** Investigation. **Giovanni Zangari:** Supervision. **Massimo Innocenti:** Conceptualization. **Francesco Vizza:** Conceptualization, Supervision, Project administration, Funding acquisition.

Declaration of Competing Interest

The authors declare that they have no known competing financial interests or personal relationships that could have appeared to influence the work reported in this paper.

Acknowledgements

We acknowledge funding of a PRIN 2017 Project funded by the Italian Ministry MUR Italy (Grant No. 2017YH9MRK). We also acknowledge the Italian Ministry MISE for the FISR 2019 Project AMPERE (FISR2019_01294).

References

[1] A. Corma, S. Iborra, A. Velty, Chemical routes for the transformation of biomass into chemicals, Chem. Rev. 107 (6) (2007) 2411–2502.

[2] R. Beerthuis, G. Rothenberg, N.R. Shiju, Catalytic routes towards acrylic acid, adipic acid and epsilon-caprolactam starting from biorenewables, Green Chem. 17 (3) (2015) 1341–1361.

[3] D.L. Sun, Y. Yamada, S. Sato, W. Ueda, Glycerol as a potential renewable raw material for acrylic acid production, Green Chem. 19 (14) (2017) 3186–3213.

[4] E.V. Makshina, J. Canadell, J. van Krieken, E. Peeters, M. Dusselier, B.F. Sels, Bio-acrylates production: recent catalytic advances and perspectives of the use of lactic acid and their derivates, ChemCatChem 11 (1) (2019) 180–201.

[5] X.K. Li, Y.G. Zhang, Highly Efficient Process for the Conversion of Glycerol to Acrylic Acid via Gas Phase Catalytic Oxidation of an Allyl Alcohol Intermediate, ACS Catal. 6 (1) (2016) 143–150.

[6] T. Murayama, B. Katryniok, S. Heyte, M. Araque, S. Ishikawa, F. Dumeignil, S. Paul, W. Ueda, Role of crystalline structure in allyl alcohol selective oxidation over Mo3VOx complex metal oxide catalysts, ChemCatChem 8 (14) (2016) 2415–2420.

[7] S. Yang, M. Kim, S. Yang, D.S. Kim, W.J. Lee, H. Lee, Production of acrylic acid from biomass-derived allyl alcohol by selective oxidation using Au/ceria catalysts, Catal. Sci. Technol. 6 (10) (2016) 3616–3622.

[8] M.V. Pagliaro, M. Bellini, M. Bevilacqua, J. Filippi, M.G. Folliero, A. Marchionni, H. A. Miller, W. Oberhauser, S. Caporali, M. Innocenti, F. Vizza, Carbon supported Rh nanoparticles for the production of hydrogen and chemicals by the electroreforming of biomass-derived alcohols, RSC Adv. 7 (23) (2017) 13971–13978.

[9] J. Mahmoudian, M. Bellini, M.V. Pagliaro, W. Oberhauser, M. Innocenti, F. Vizza, H.A. Miller, Electrochemical coproduction of acrylate and hydrogen from 1,3-Propandiol, ACS Sustain. Chem. Eng. 5 (7) (2017) 6090–6098.

[10] M.V. Pagliaro, M. Bellini, J. Filippi, M.G. Folliero, A. Marchionni, H.A. Miller, W. Oberhauser, F. Vizza, Hydrogen production from the electrooxidation of methanol and potassium formate in alkaline media on carbon supported Rh and Pd nanoparticles, Inorg. Chim. Acta 470 (2018) 263–269.

[11] M. Bellini, M.V. Pagliaro, A. Marchionni, J. Filippi, H.A. Miller, M. Bevilacqua, A. Lavacchi, W. Oberhauser, J. Mahmoudian, M. Innocenti, P. Fornasiero, F. Vizza, Hydrogen and chemicals from alcohols through electrochemical reforming by Pd-CeO2/C electrocatalyst, Inorg. Chim. Acta 518 (2021), 120245.

[12] L.Q. Wang, A. Lavacchi, M. Bevilacqua, M. Bellini, P. Fornasiero, J. Filippi, M. Innocenti, A. Marchionni, H.A. Miller, F. Vizza, Energy efficiency of alkaline direct ethanol fuel cells employing nanostructured palladium electrocatalysts, ChemCatChem 7 (14) (2015) 2214–2221.

[13] V. Bambagioni, C. Bianchini, Y.X. Chen, J. Filippi, P. Fornasiero, M. Innocenti, A. Lavacchi, A. Marchionni, W. Oberhauser, F. Vizza, Energy efficiency enhancement of ethanol electrooxidation on Pd-CeO2/C in passive and active polymer electrolyte-membrane fuel cells, ChemSusChem 5 (7) (2012) 1266–1273.

[14] Y.X. Chen, A. Lavacchi, H.A. Miller, M. Bevilacqua, J. Filippi, M. Innocenti, A. Marchionni, W. Oberhauser, L. Wang, F. Vizza, Nanotechnology makes biomass electrolysis more energy efficient than water electrolysis, Nat. Commun. 5 (2014).

[15] H.A. Miller, A. Lavacchi, F. Vizza, M. Marelli, F. Di Benedetto, F.D.I. Acapito, Y. Paska, M. Page, D.R. Dekel, A Pd/C-CeO2 anode catalyst for high-performance platinum-free anion exchange membrane fuel cells, Angew. Chem. Int. Ed. 55 (20) (2016) 6004–6007.

[16] H.A. Miller, F. Vizza, M. Marelli, A. Zadick, L. Dubau, M. Chatenet, S. Geiger, S. Cherevko, H. Doan, R.K. Pavlicek, S. Mukerjee, D.R. Dekel, Highly active nanostructured palladium-ceria electrocatalysts for the hydrogen oxidation reaction in alkaline medium, NANO Energy 33 (2017) 293–305.

[17] L.Q. Wang, A. Lavacchi, M. Bellini, F. D`Acapito, F. Di Benedetto, M. Innocenti, H. A. Miller, G. Montegrossi, C. Zafferoni, F. Vizza, Deactivation of palladium electrocatalysts for alcohols oxidation in basic electrolytes, Electrochim. Acta 177 (2015) 100–106.

[18] G. Sabitha, S. Nayak, M. Bhikshapathi, J.S. Yadav, Palladium hydroxide catalyzed isomerization of primary allylic alcohols to aldehydes: application to the formal synthesis of (-)-Brevisamide, Org. Lett. 13 (3) (2011) 382–385.

[19] C. Bianchini, A. Meli, W. Oberhauser, Isomerization of allylic alcohols to carbonyl compounds by aqueous-biphase rhodium catalysis, New J. Chem. 25 (1) (2001) 11–12.

[20] J. Muzart, Palladium-catalysed oxidation of primary and secondary alcohols, Tetrahedron 59 (31) (2003) 5789–5816.

[21] P. Lorenzo-Luis, A. Romerosa, M. Serrano-Ruiz, Catalytic Isomerization of allylic alcohols in water, ACS Catal. 2 (6) (2012) 1079–1086.

[22] R.C. van der Drift, E. Bouwman, E. Drent, Homogeneously catalysed isomerisation of allylic alcohols to carbonyl compounds, J Organomet Chem 650 (1–2) (2002) 1–24.